

# A Comparative Study of Different Feature Extraction Methods for Motor Imagery EEG Decoding within the Same Upper Extremity

Yaqi Chu<sup>1,2,3</sup>, Xingang Zhao<sup>1,2</sup>, Yijun Zou<sup>1,2,3</sup>, He Zhang<sup>5</sup>, Weiliang Xu<sup>1,4</sup>, and Yiwen Zhao<sup>1,2</sup>

<sup>1</sup>State Key Laboratory of Robotics, Shenyang Institute of Automation (SIA),  
Chinese Academy of Sciences (CAS)  
Shenyang, Liaoning, 110016, China

{chuyaqi, zhaoxingang, zouyijun, zhaoyw}@sia.cn

<sup>2</sup>Institutes for Robotics and Intelligent Manufacturing,  
Chinese Academy of Sciences (CAS)  
Shenyang, Liaoning, 110016, China

<sup>3</sup>University of Chinese Academy of Sciences (UCAS)  
Beijing, 100049, China

<sup>4</sup>Department of Mechanical Engineering  
University of Auckland  
Auckland, 1142, New Zealand  
p.xu@auckland.ac.nz

<sup>5</sup>Department of Orthopedics, Xinqiao Hospital  
Third Military Medical University  
Chongqing, 400038, China  
alafiam@163.com

**Abstract**—Compared to other electroencephalogram (EEG) modalities, motor imagery (MI) based brain-computer interfaces (BCIs) can provide more natural and intuitive communication between human intentions and external machines. However, this type of BCI depends heavily on effective signal processing to discriminate EEG patterns corresponding to various MI tasks, especially feature extraction procedures. In this study, a comparison of different feature extraction methods was conducted for EEG classification of imaginary movements within the same upper extremity. Unlike traditional MI tasks (left/right hand), six imaginary movements from the same unilateral upper extremity were proposed and evaluated, including elbow extension/flexion, wrist pronation/supination, and hand open/grasp. To tackle the classification challenge of MI tasks within the same limb, four types of feature extraction methods were implemented and compared in combination with support vector machine (SVM) and linear discriminant analysis (LDA) classifiers, such as wavelet transformation, power spectrum, autoregressive model, common spatial patterns (CSP) and variants of filter-bank CSP (FBCSP), regularized CSP (RCSP). The overall accuracies of the CSP were significant higher than other three types of feature extraction on a dataset collected from 8 individuals, particularly the SVM with FBCSP had the best performance with an average accuracy of 71.78%. These decoding results of MI tasks during single upper extremity are encouraging and promising in the context of more natural MI-BCI for controlling assisted devices, such as a neuroprosthetic or robotic arm for motor disabled individuals with highly impaired upper extremity.

**Keywords**—motor imagery EEG, same upper extremity, feature extraction, common spatial patterns, brain-computer interface.

## I. INTRODUCTION

Non-invasive brain-computer interfaces (BCIs) based on electroencephalogram (EEG) provide a promising pathway for the development of an interactive control of a robotic device or a neural prosthesis to assist motor disabled persons [1, 2], especially for the EEG modality of motor imagery (MI) [3, 4]. MI-based BCIs decode a specific mental activity into control command by power modulations of sensorimotor rhythms, such as the event-related de/synchronization (ERD/ERS) activity [5, 6]. Compared to steady-state visual evoked potential (SSVEP) [7] or P300, the MI-based BCIs are more useful and flexible in view of natural and intuitive interaction.

A variety of MI-based BCIs were developed in different fields, such as control of wheelchairs [8], prosthetic arms or devices [9], mobile and humanoid robots [10], mind-driven navigation in gaming or virtual reality [11]. However, most MI-based BCIs can only discriminate a finite number of MI tasks (usually two or three) and decode spatially well separated MI patterns in brain areas as control commands. For example, left/right hand, foot and/or tongue MI tasks are the most commonly adopted among the MI-based BCI systems [6, 12]. Due to the fact that MI tasks within the same upper extremity activate and occupy the same brain regions on the motor cortex area [13, 14], the EEG signals have non-stationary and overlapped representations, which makes them really challenging to detect the MI tasks from the same limb.

This research was funded by the Nation Natural Science Foundation of China (Grants nos. 61503374 and 61573340), and supported by the Frontier Science research project of the Chinese Academy of Sciences (Grant No. QYZDY-SSW-JSC005).

There are relatively few researches that address the recognition challenge of various MI tasks from the same limb. Vuckovic and Sepulveda combined an Elman neural network classifier with time-frequency features to detect four real and imaginary wrist motions (supination/pronation and extension/flexion), with 71.3% accuracy for each pair [15, 16]. Similarly, Edelman *et al.* adopted source space analysis method with band power features to promote the decoding performance of imaginary wrist motions with an average accuracy of 81.4% [17]. Liao *et al.* applied a support vector machine (SVM) classifier with power spectral features to decode ten pairs of finger motion intents by EEG [18]. Menon *et al.* conducted a preliminary comparison of nine various schemes to decode rest and two MI tasks (hand grasp and elbow) for the identical limb, employing three state-of-the-art feature extraction with an average accuracy of 58.4% [14]. In a further study, a decoding scheme of integrating optimal SVM with time-domain features was proposed to improve the performance of 3-class BCI with 74.2% accuracy, including autoregressive (AR) model coefficients, waveform length (WL) and root mean square (RMS) [19]. Ofner *et al.* investigated the decoding of executed/imagined movements by using time-domain features of the low frequency EEG for single upper limb, with accuracy of 55% for executed movements, 27% for imagined movements [20]. From the above studies, we can see that the decoding accuracy and feasibility of the MI-based BCIs highly relies on EEG signal processing for the different MI tasks within the same limb, particularly feature extraction procedures.

In view of EEG signals have relative low spatial resolution and signal-to-noise ratio, an effective signal processing scheme is extremely important. Furtherly, the decoding performance was extremely affected by the extracted features. Currently, massive feature extraction methods and classifiers have been developed and applied to EEG recognition for MI-based BCIs [21, 22]. Some widely used feature extraction methods have been implemented in the traditional MI tasks (left/right hand), including power spectral analysis [23], wavelet transformation [24], AR model [25], common spatial pattern (CSP) and variants of filter-bank CSP (FBCSP), regularized CSP (RCSP), sub-band CSP (SBCSP) [26]. However, for the MI tasks within the same limb, there are few comparison studies by using those state-of-the-art feature extraction methods.

In this paper, a comparative study for decoding multiple MI tasks within the same limb was evaluated by combining four types of feature extraction methods with SVM and linear discriminant analysis (LDA), including wavelet transformation, power spectrum, AR model, and CSP (FBCSP, RCSP). Six imaginary movements from the same upper extremity were designed, including elbow extension/flexion, forearm or wrist pronation/supination, and hand open/grasp (similar to [20]).

The entire structure of this paper consists of the following parts. The systematic method for MI decoding is introduced in Section II. The MI experiment and datasets are presented in Section III. Section IV describes detailed signal processing methodology. Then, experimental results and discussions are showed in Section V. Finally, Section VI gives the conclusions and future works.

## II. OVERALL DECODING FRAMEWORK

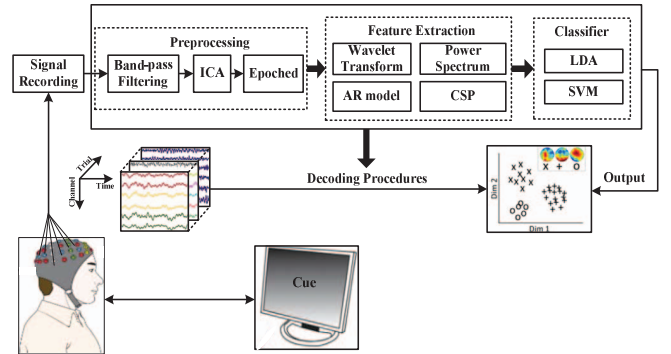


Fig. 1. The integral decoding framework for various MI EEG from the same limb by using different feature extraction methods and classifiers.

The theme of our study is to compare the performance of different feature extraction methods for decoding MI EEG elicited by the same upper extremity. The decoding framework of the integral scheme is presented in Fig. 1, which mainly includes three parts: raw MI EEG preprocessing, four types of feature extraction methods, and two classifiers. The raw MI EEG was recorded by using non-invasive electrodes with wet gel when subjects do diverse imaginary motion intents with their ipsilateral limbs. The preprocess procedure was adopted to construct pure MI EEG datasets, including band-pass filtering, independent component analysis (ICA), and sliding windows segmentation. Different domains of features were retrieved by power spectrum (frequency domain), AR model (time domain), wavelet transform (time-frequency domain) and CSP (spatial domain). The extracted features were separately fed to SVM and LDA to discriminate the various MI tasks within the same limb. The results were comparatively evaluated and analyzed in the aspect of feature extraction and classifier individually.

## III. MOTOR IMAGERY EEG DATASETS

### A. Subjects

Eight normal individuals (right-handed, age range from 23 to 26 years old, all males, named S01-S08) were recruited to participate the MI research. All individuals have no any disease history, especially for the cognitive or neurological dysfunction. Explicitly, none of them has never experienced the MI experiment. Written informed consent was signed, and the experiment was approved by the ethics committee of the Third Military Medical University.

### B. Experimental Paradigm

According to [20], six imaginary movements (shown in Fig. 2) from the same limb were designed for three joints (elbow, wrist and hand). In the electrical and magnetic shielding condition, the individuals sat in a chair and looked at a computer screen in the front distance with rough 1.5 m. The trial-based cues were displayed in this experimental paradigm. Before the start of the experiments, the upper extremity was at a neutral position: the forearm extended to 120 degrees, the hand relaxed and palm half opened, and wrist in a neutral rotation.

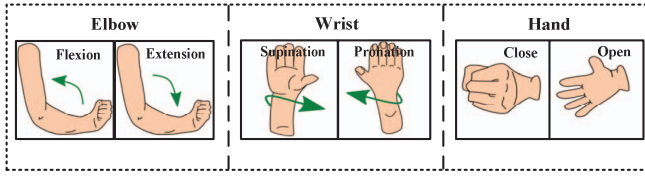


Fig. 2. The diagram of six imaginary motions from the same limb.

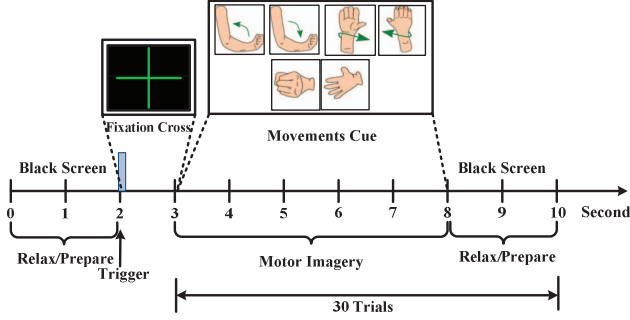


Fig. 3. The motor imagery EEG paradigm.

The experiment consists of 10 sessions with the total duration of one hour. All sessions were implemented during the same condition with a break of ten minutes between the two consecutive sessions. Figure 3 shows the sequence of the paradigm in a session. The 2 s black screen was a relax/prepare period before the triggers. Then, at the center of the computer screen, a cross with green color was appeared to give an indication, which last 1 s. Immediately, a movement cue (a figure in Fig. 2) displayed on the screen with duration of 5 s. According to the cue information, the individual was recommended to conduct relevant MI tasks within the same upper extremity respectively during that time period, such as repeatedly imaginary kinesthetic grasp of hand. In addition, to minimize the artefacts that may arise by the subjects, the trier should not to blink or swallow and try not to move their body. At the end of the trial, the subjects perform relax/prepare state and hold back to the neutral position. Each of the cues was presented by a randomized order. In each session, 30 trials were recorded with 5 trials for each class. For each individual in an experiment, the total MI tasks are 300 trials with 5 s length.

### C. Recording and Dataset

A 64-channels grid cap with Ag/AgCl scalp electrode produced by Plexon Inc., USA was used to record the EEG. The 64 channels were arranged according to the international 10-20 positioning system. The right mastoid channel was regarded as ground and the left mastoid channel served as reference. The recorded analog signal was transformed by pre-amplification, a low-pass filter and A/D conversion, which provided by OmniPlex Acquisition System (Plexon Inc.). Additionally, the power line interference was removed by using a notch filter with 60 Hz. The MI EEG signals were sampled at 1 kHz and stored as  $64 \times 5000 \times 300$  (a form of channels  $\times$  times  $\times$  trials). To obtain most representative MI EEG, a 4 s period was cut out from each trial. Hence, the MI EEG signal sets were established by a three-dimensional array with  $64 \times 4000 \times 300$  size for each subject. The 75% signal sets were randomly selected as training set and the rest was testing set.

## IV. DECODING METHODOLOGY

### A. EEG Preprocessing

To eliminate the unwanted parts of the MI EEG, the preprocessing module was applied, including a) band-pass filtering, b) ICA and c) sliding windows segmentation.

1) *Band-pass filtering*: For MI signals, the ERS/ERD phenomenon usually presents in the 8-30 Hz frequency band, such as mu (8-12 Hz) and beta (18-26 Hz) rhythms [6]. This frequency band has the maximal information related to MI tasks. To attenuate the specific artifacts while amplify interested 8-30 Hz frequency component, a Butterworth band-pass filter (cutoff frequency of 8 Hz and 35 Hz) with fifth-order was adopted. Then, a large part of EMG (higher than 35 Hz) and electrical line interference (50-60 Hz) was removed.

2) *ICA*: To remove EOG, an ICA procedure was adopted. The EEG signals were decomposed into multiple independent components (ICs) based on high order statistics. By visual inspection, some ICs corresponding to EOG artefacts were rejected. The selected non-artefactual ICs were mixed and projected back onto the original channel space to obtain the EOG-free EEG signals. In this study, 32 ICs were isolated from EEG signals for each subject by using FastICA algorithm of the EEGLAB software [27].

3) *Sliding windows segmentation*: The MI EEG period should be segmented to improve the temporal resolution. Moreover, a trial of MI tasks need repeatedly envision body motions for a while to produce steady and stable rhythm modulation. Hence, in this paper, a sliding window method was used to divide trial-based EEG into overlapped segments. For a four-second period of motor imagery EEG signals, a 1 s sliding window with 80 % overlap was used to spilt into 16 segments with 1 s length. Hence, for each subject, the dataset was  $64 \times 1000 \times 4800$ , where 4800 was the number of epoch signal.

### B. Different Feature Extraction Methods

The core of a MI-based BCI/BMI is feature extraction, which highlights important information corresponding to MI and eliminate non-informative parts. To compare the performance, four types of feature extraction methods were adopted, including AR model, power spectrum, wavelet transform and CSP. A MI EEG epoch can be written by  $\mathbf{X} \in R^{C \times N}$ , where  $C$  represents the channel number and  $N$  is the sample length. For every electrode, the MI EEG time sequence was represented by  $eeg_t$ , where  $t = 1, 2, \dots, N$ .

1) *AR model*: The classical AR model is a time-domain analysis method, which depicts time-varying features of EEG signals. AR model provides information regarding previous samples by a weighted linear combination of samples in a segment. The time resolution and accuracy of AR model depend on the length of the signal segment. A shorter length can bring a higher resolution and result in a larger estimation error of the model. To solve the problem, an adaptive AR (AAR) model was used in this paper. The mathematical formula of AAR model is given as follows:

$$eeg_t = \alpha_{1,t} eeg_{t-1} + \alpha_{2,t} eeg_{t-2} + \dots + \alpha_{p,t} eeg_{t-p} + \mathcal{E}_t, \quad (1)$$

where  $\alpha_{i,t}$  ( $i=1, \dots, p$ ) are coefficients of the AAR model,  $p$  is the order ( $p=4$  in this study) and  $\mathcal{E}_t$  is the white noise. The 4 model coefficients estimated by a recursive least square (RLS) algorithm were used to represent the EEG features.

2) *Power spectrum*: The power spectrum method is mainly used to extract band energy features, which represent the ERD/ERS variation in the frequency domain. The power features can be obtained by a direct method (fast Fourier transform, FFT). However, since the EEG signal is non-periodic, the FFT estimation cannot conform consistent estimation condition and readily generate spectrum leakage. In this study, the welch method was used to estimate the frequency spectrum. For MI EEG mostly located in 8-30 Hz, four sub-bands were divided by a 6 Hz bandwidth, including high beta (23-28 Hz) and low beta (18-23 Hz), sigma (13-18 Hz), and alpha (8-13 Hz) rhythms. The power spectral features during each sub-band were obtained for each channel, using averaging powers by welch method.

3) *Wavelet transform*: The wavelet transform provides an effective solution for non-stationary EEG signal to extract time-frequency features. Moreover, the discrete wavelet transform (DWT) can produce fine temporal and spectral analysis by using different contracted and dilated versions of the wavelet base. The DWT decomposes signals into detailed and approximate coefficients by successive high pass and low pass filtering created by orthonormal wavelet bases. These coefficients span different non-overlapping sub-bands for the EEG signals. In this study, a 2-level DWT with gabor wavelet was adopted to divide the 8-30 Hz MI EEG into four sub-bands, including 8-13.5 Hz, 13.5-19 Hz, 19-24.5 Hz and 24.5-30 Hz. The power features were computed by averaging the sum of the signals reconstructed from the coefficients within each sub-band.

4) *CSP*: The common spatial pattern (CSP) is an effective spatial filter to extract features for discriminating two classes of EEG signals related to MI tasks. For two classes of MI EEG,  $\mathbf{x}_j^k \in \mathbf{X}$  denotes the  $j$ -th EEG segment from the  $k$  class ( $k=1, 2$ ). The corresponding spatial covariance matrix  $\Sigma$  is computed by

$$\Sigma_k = \frac{1}{N_k} \sum_{j=1}^{N_k} \mathbf{x}_j^k (\mathbf{x}_j^k)^T, \quad (2)$$

where  $N_k$  is the number of EEG segments in class  $k$ . The spatial filters of CSP are learned and computed by maximizing the below ratio formula:

$$\max_{\mathbf{w}} \mathbf{J}(\mathbf{w}) = \frac{\mathbf{w}^T \Sigma_1 \mathbf{w}}{\mathbf{w}^T \Sigma_2 \mathbf{w}} \quad s.t. \quad \|\mathbf{w}\|_2 = 1, \quad (3)$$

where  $\mathbf{w} \in \mathbf{R}^C$  is a spatial matrix, and  $\|\bullet\|_2$  represent  $l_2$ -norm. By solving the generalized eigenvalue decomposition problem, the relevant eigenvectors can be obtained to form  $\mathbf{w}$ .

$$\Sigma_1 \mathbf{w} = \lambda \Sigma_2 \mathbf{w} \quad (4)$$

Generally, the  $e$  eigenvectors corresponding to the highest and the lowest eigenvalues are selected to construct spatial filtering matrix  $\tilde{\mathbf{w}} \in \mathbf{R}^{C \times S}$ ,  $S = 2 \times e$ . The projection of a given EEG  $\mathbf{X}$  is given by

$$\mathbf{Z} = \tilde{\mathbf{w}}^T \mathbf{X}. \quad (5)$$

Then the spatial feature vector is formed as  $\mathbf{f} = [f_1, \dots, f_S]$  by

$$f_m = \log \left( \frac{\text{var}(\mathbf{Z}_m)}{\sum_{m=1}^S \text{var}(\mathbf{Z}_m)} \right), \quad (6)$$

where  $\text{var}(\bullet)$  and  $\log(\bullet)$  denote the variance, logarithm operator respectively.

Due to the CSP for solving two class problem, a One-vs-Rest strategy was applied to cope with multi-class MI EEG. In this study, for six MI classes, there were six CSP filters. For each CSP, the number of selected eigenvectors is  $e=2$ . Hence, the total spatial filtering matrix is  $\mathbf{W} \in \mathbf{R}^{C \times S}$ , where  $S = 2 \times e \times 6$  is the number of CSP projections. In addition, FBCSP and RCSP were also introduced in the comparison study. For FBCSP, three frequency bands 8-16 Hz, 17-25 Hz, and 26-32 Hz were separately used to filter EEG. In summary, for each EEG epoch, 24, 72, and 24 spatial features were extracted for CSP, FBCSP, and RCSP, respectively.

### C. Classification

Considering the performance and computation complexity, two efficient state-of-the-art classifiers (LDA and SVM) were used in this paper.

1) *LDA*: The commonly adopted classifier in BCI systems is the LDA, which aims to find a linear hyperplane to characterize or separate two classes of MI EEG signals. More explicitly, this hyperplane or projection is optimized by maximizing inter-class divergence and minimizing intra-class divergence synchronously. Since LDA is a binary classifier, a One-vs-One strategy was conducted to address multiple class classification. In this paper, the class of MI EEG was assigned using a maximum voting way from 15 LDA classifiers.

2) *SVM*: The SVM executes in a similar manner with LDA, by attempting to search a high-dimensional hyperplane to discriminate samples with a maximum margin. The generalization capabilities of the SVM are increased by maximizing this margin. The hyperplane can be obtained by solving the following optimization problem:

$$\min_{\mathbf{w}, \mathbf{b}} \frac{1}{2} \|\mathbf{W}\|^2 + c \sum_{i=1}^N \zeta_i \quad s.t.: \quad y_i (\mathbf{W}^T x_i + \mathbf{b}) \geq 1 - \zeta_i, \quad \zeta_i \geq 0 \quad (7)$$

where  $c$  is a regularization term,  $\zeta_i$  are slack parameters,  $x_i$  is the feature vector representing a sample,  $y_i$  is the associated label,  $i$  is the sample index. With the use of a kernel function which mapped the sample to higher dimensional space, an optimized hyperplane can be used to easily separate the mapped sample. In this study, a radial basis function (RBF) was selected as the kernel function. The kernel parameter and regularization

term  $C$  were optimized by a grid search in the range of (0, 5). Furthermore, a 5-fold cross-validation procedure was used to prevent over-fitting for training a classifier.

## V. EXPERIMENT RESULTS AND DISCUSSIONS

### A. Comparison with different feature extraction methods

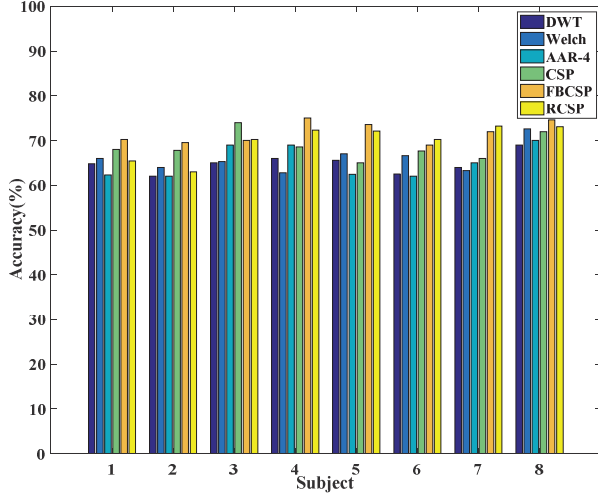


Fig. 4. The accuracy of SVM with different feature extraction methods for eight subjects, respectively.

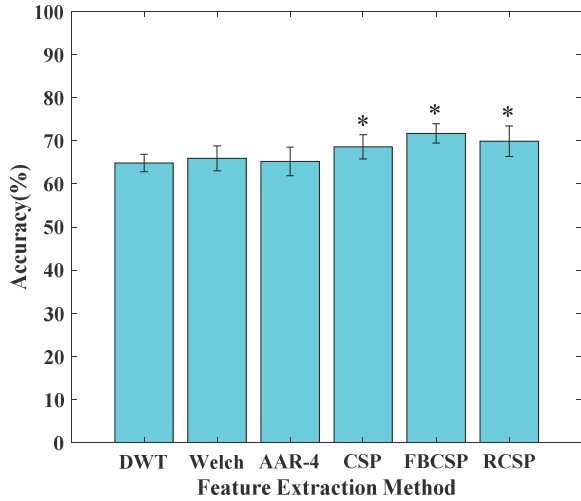


Fig. 5. The average performance (mean  $\pm$  standard deviation) of different feature extraction methods across eight subjects.

Six feature extraction methods (DWT, Welch, AAR-4, CSP, FBCSP, and RCSP) were individually applied for the eight subjects' datasets. The extracted features were fed to the SVM classifiers. The classification accuracy of SVM with six types of feature datasets were show in Fig. 4. It illustrates that the CSP, FBCSP, and RCSP methods have higher performance for each subjects compared to the DWT, Welch, and AAR-4 methods. More specifically, the average classification performance (mean  $\pm$  standard deviation) for each feature extraction method is presented in Fig. 5. The DWT, Welch, AAR-4, CSP, FBCSP, and RCSP produced a mean accuracy of  $64.86 \pm 2.05\%$ ,  $65.95 \pm 2.90\%$ ,  $65.22 \pm 3.32\%$ ,  $68.63 \pm 2.79\%$ ,  $71.73 \pm 2.24\%$ ,  $69.94 \pm 3.59\%$  respectively. The analysis of

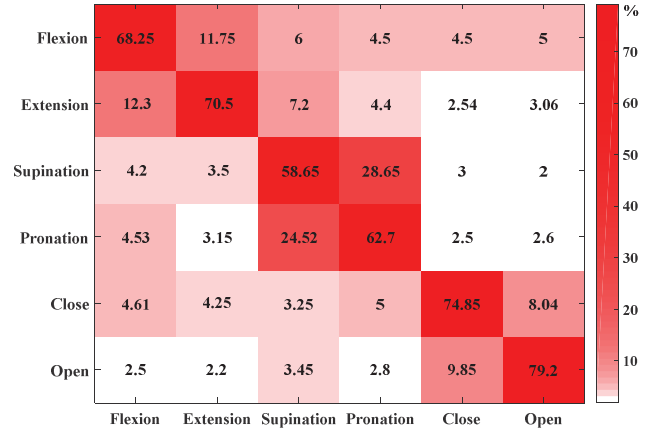


Fig. 6. The accuracy confusion matrix for six classes of MI tasks obtained by SVM classifier with FBCSP methods.

variance (ANOVA) was carried out to show the statistically significant difference of six methods. The DWT, Welch, and AAR-4 methods have no significant difference for the average accuracy ( $p$ -value  $> 0.76$ ). However, there is a significant difference ( $p$ -value  $< 0.05$ ) using Kruskal-Wallis test between DWT, Welch, AAR-4 and CSP, FBCSP, RCSP. Especially, the FBCSP method has the best classification accuracy with lower deviation ( $p$ -value  $< 0.01$ ). This result might be attributed to the improved spatial separability of the FBCSP algorithm.

Furthermore, Fig. 6 shows an accuracy confusion matrix obtained by SVM classifier with FBCSP, corresponding to joint movements-level classification results for six MI tasks. The average accuracy was 68.25%, 70.5%, 58.65%, 62.70%, 74.85%, and 79.20% for flexion/extension (elbow joint), supination/pronation (elbow and wrist joint), and close/open (hand), respectively. Interestingly, the distribution of false recognition rates is obviously non-uniform for each paired-MI tasks. Particularly, the classification accuracies for supination/pronation MI tasks were lower with notable misclassification errors than that of other MI tasks. The possible reason may be the fact that the supination/pronation MI tasks derived from multiple joints within the same limb are tightly emerged at the adjacent sensorimotor cortex. So, the spatial separability of the relevant EEG signals is ambiguous.

### B. Comparison between LDA and SVM

Moreover, for the features extracted by the FBCSP methods, the comparison analysis of LDA and SVM classifiers were conducted. The accuracies of the two classifiers for each individual and mean accuracies are presented in Fig. 7. Generally, the performance of the SVM is slightly better than that of LDA for each subject. The mean accuracy is  $69.02\% (\pm 1.65\%)$  for LDA and  $71.78\% (\pm 1.92\%)$  for SVM. The post hoc test using the Kruskal-Wallis method indicates a statistically significant difference in classification accuracy between LDA and SVM, with  $p$ -value =  $0.012 < 0.05$ . The increased performance of SVM classifier is benefited by the improved generalization capabilities and maximized separable margins using optimal parameters.

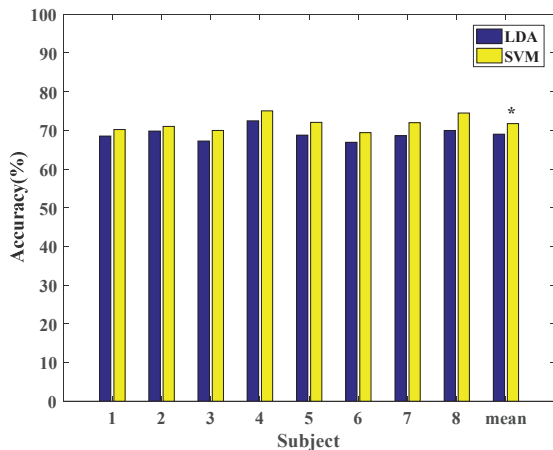


Fig. 7. The accuracy of LDA and SVM classifier for eight subjects.

## VI. CONCLUSIONS AND FUTURE WORKS

In this paper, we carried out a comparative study for decoding six motor imagery EEG within the same upper extremity by using four types of feature extraction methods and two classifiers (LDA and SVM), including wavelet transformation, power spectrum, AR model, and CSP (FBCSP, RCSP). The CSP algorithm was better than the other three methods, especially for the FBCSP and RCSP methods. Compared to the LDA, the SVM classifier was more suitable and effective for decoding various MI tasks within the same limb, such as elbow extension/flexion, wrist pronation/supination, and hand open/grasp. For these MI tasks, the highest overall performance of the SVM with FBCSP was obtained, with accuracy of 71.78% ( $\pm 1.92\%$ ). In the future work, the decoding method could potentially be applied in BCI-driven assistive robots or neuroprosthetics by using natural and intuitive motor imagery EEG signals.

## ACKNOWLEDGMENTS

This study was funded by the Nation Natural Science Foundation of China (Grants nos. 61503374 and 61573340), and supported by the Frontier Science research project of the Chinese Academy of Sciences (Grant No. QYZDY-SSW-JSC005). The authors would appreciate Yingli Li *et al.* for participating the MI experiments.

## REFERENCES

- [1] S. Gao, Y. Wang, X. Gao, and B. Hong, "Visual and auditory brain-computer interfaces," *IEEE Trans. Biomed. Eng.*, vol. 61, no. 5, pp. 1436-1447, 2014
- [2] L. R. Hochberg, D. Bacher, B. Jarosiewicz, N. Y. Masse, J. D. Simeral, J. Vogel, *et al.*, "Reach and grasp by people with tetraplegia using a neurally controlled robotic arm," *Nature*, vol. 485, pp. 372-375, 2012
- [3] H. Yuan and B. He, "Brain-computer interfaces using sensorimotor rhythms: current state and future perspectives," *IEEE Trans. Biomed. Eng.*, vol. 61, no. 5, pp. 1425-1435, 2014
- [4] B. He, B. Baxter, B. J. Edelman, C. C. Cline, and Wenjing W. Ye, "Noninvasive brain-computer interfaces based on sensorimotor rhythms," *Proc. IEEE*, vol. 103, no. 6, pp. 907-925, 2015
- [5] G. Pfurtscheller, C. Brunner, A. Schlögl, and F. Lopes da Silva, "Mu rhythm (de)synchronization and EEG single-trial classification of different motor imagery tasks," *NeuroImage*, vol. 31, no. 1, pp. 153-9, 2006

- [6] J. Wagner, S. Makeig, M. Gola, C. Neuper, and G. R. Müller-Putz, "Distinct  $\beta$  band oscillatory networks subserving motor and cognitive control during gait adaptation," *J. Neurosci.*, vol. 36, pp. 2212-2226, 2016
- [7] X. Zhao, Y. Chu, J. Han, and Z. Zhang, "SSVEP-based brain-computer interface controlled functional electrical stimulation system for upper extremity rehabilitation," *IEEE Trans. Syst. Man, Cybern. Syst.*, vol. 46, pp. 947-956, 2016
- [8] G. Reshmi, and A. Amal, "Design of a BCI System for Piloting a Wheelchair Using Five Class MI Based EEG," In: *2013 Third International Conference on Advances in Computing and Communications (ICACC)*, pp. 25-28, 2013
- [9] Y. N. Li, X. D. Zhang, and Z. X. Huang, "A practical method for motor imagery based real-time prosthesis control," In: *2012 IEEE International Conference on Automation Science and Engineering*, Seoul, pp. 1052-1056, 2012
- [10] Y. Chae, J. Jeong, and S. Jo, "Toward brain-actuated humanoid robots: asynchronous direct control using an EEG-based BCI," *IEEE Trans. Robotics*, vol. 28, no. 5, pp. 1131-1144, 2012
- [11] D. Coyle, J. Garcia, A. R. Satti, and T. M. McGinnity, "EEG-based continuous control of a game using a 3 channel motor imagery BCI: BCI game," In: *2011 IEEE Symposium on Computational Intelligence, Cognitive Algorithms, Mind, and Brain (CCMB)*, Paris, 2011
- [12] T. Geng, M. Dyson, C. S. Tsui, and J. Q. Gan, "A 3-class asynchronous BCI controlling a simulated mobile robot," In: *2007 IEEE Conference on Proceedings of the Engineering in Medicine and Biology Society (EMBS)*, Lyon, pp. 2524-2527, 2007
- [13] E. B. Plow, P. Arora, M. A. Pline, M. T. Binenstock, and J. R. Carey, "Within-limb somatotopy in primary motor cortex—revealed using fMRI," *Cortex*, vol. 46, no. 3, pp. 310-321, 2010
- [14] X. Yong, and C. Menon, "EEG classification of different imaginary movements within the same limb," *PLoS One*, vol. 10, e0121896, 2015
- [15] A. Vuckovic, and F. Sepulveda, "Delta band contribution in cue based single trial classification of real and imaginary wrist movements," *Med. Biol. Eng. Comput.*, vol. 46, no. 6, pp. 529-539, 2008
- [16] A. Vuckovic, and F. Sepulveda, "A two-stage four-class BCI based on imaginary movements of the left and the right wrist," *Med. Eng. Phys.*, vol. 34, no. 7, pp. 964-971, 2012
- [17] B. J. Edelman, B. Baxter, and B. He, "EEG source imaging enhances the decoding of complex right-hand motor imagery tasks," *IEEE Trans. Biomed. Eng.*, vol. 63, no. 1, pp. 4-14, 2016
- [18] K. Liao, R. Xiao, J. Gonzalez, and L. Ding, "Decoding individuals finger movements from one hand using human EEG signals," *PLoS One*, vol. 9, no. 1, e85192, 2014
- [19] M. Tavakolan, Z. Frehlick, X. Yong, and C. Menon, "Classifying three imaginary states of the same upper extremity using time-domain features," *PLoS One*, vol. 12, no. 3, e0174161, 2017
- [20] P. Ofner, A. Schwarz, J. Pereira, and G. R. Müller-Putz, "Upper limb movements can be decoded from the time-domain of low-frequency EEG," *PLoS One*, vol. 12, no. 8, e0182578, 2017
- [21] F. Lotte, L. Bougrain, A. Cichocki, M. Clerc, M. Congedo, A. Rakotomamonjy, *et al.*, "A review of classification algorithms for EEG-based brain-computer interfaces: a 10 year update," *J. Neural Eng.*, vol. 15, no. 3, 031005, 2018
- [22] R. V. Wankar, P. Shah, and R. Sutar, "Feature extraction and selection methods for motor imagery EEG signals: A review," In: *2017 International Conference on Intelligent Computing and Control (I2C2)*, Coimbatore, pp. 1-9, 2017
- [23] P. Herman, G. Prasad, T. M. McGinnity, and D. Coyle, "Comparative analysis of spectral approaches to feature extraction for EEG-based motor imagery classification," *IEEE Trans. Neural Syst. Rehabil. Eng.*, vol. 16, no. 4, pp. 317-326, 2008
- [24] R. Yang, A. Song, and B. Xu, "Feature extraction of motor imagery EEG based on wavelet transform and higher-order statistics," *Int. J. Wavelets Multiresolut. Inf. Process.*, vol. 8, no. 3, pp. 373-384, 2010
- [25] K. Inoue, D. Mori, G. Pfurtscheller, and K. Kumamaru, "Pattern recognition of EEG signals during right and left motor imagery," *Complex Medical Engineering*, Springer, Tokyo, pp. 251-261, 2007
- [26] Y. Zhang, G. Zhou, J. Jin, X. Wang, and A. Cichochi, "Optimizing spatial patterns with sparse filter bands for motor-imagery based brain-computer interface," *J. Neurosci. Methods*, vol. 255, pp. 85-91, 2015
- [27] A. Delorme and S. Makeig, "EEGLAB: an open source toolbox for analysis of single-trial EEG dynamics," *J. Neurosci. Methods*, vol. 134, no. 1, pp. 9-21, 2004